

ICPES 2025

40th INTERNATIONAL CONFERENCE ON PRODUCTION ENGINEERING - SERBIA 2025

DOI: <u>10.46793/ICPES25.439T</u>



University of Nis
Faculty of Mechanical
Engineering

Nis, Serbia, 18 - 19th September 2025

RELATIONSHIP BETWEEN POROSITY AND MECHANICAL PERFORMANCE OF CUSTOM LATTICE-LIKE BONE SCAFFOLDS

Rajko TURUDIJA^{1*}, Jovan ARANĐELOVIĆ¹, Miloš STOJKOVIĆ¹, Jelena STOJKOVIĆ¹, Nikola KORUNOVIĆ¹

 $\textbf{Orcid:}\ 0000-0002-6324-5967;\ \textbf{Orcid:}\ 0000-0001-9653-4119;\ \textbf{Orcid:}\ 0000-0001-9020-125X;$

*Corresponding author: rajko.turudija@masfak.ni.ac.rs

Abstract: Bone scaffolds for the treatment of large defects serve two primary functions: to replicate the mechanical properties of natural bone, particularly elasticity, thereby preventing complications such as stress shielding and implant failure, and to promote bone regeneration by incorporating bioactive agents that stimulate new tissue growth. To retain these substances in place and to prevent their diffusion or migration away from the targeted site, scaffolds must be sufficiently porous to allow substance delivery and vascularization but also mechanically stable enough to replicate the properties of the bone region they are intended for. This work presents an analysis of experimental results obtained by mechanical testing of custommade lattice-like scaffolds, focusing on their porosity and mechanical performance. Porosity of scaffolds was varied by varying the design parameters of a custom CAD model of lattice-like scaffold (such as strut diameter, strut angle, etc.). These scaffolds were fabricated using SLS 3D printing technology and tested under uniaxial compression using a universal testing machine. The results reveal an almost linear negative correlation between scaffold porosity and compressive strength, which aligns with theoretical expectations. It was also observed that scaffolds with very similar porosity values (e.g., 76% vs. 77%) can exhibit significant differences in mechanical strength, with the difference sometimes exceeding 600 N, indicating that strut arrangement and geometry also play a crucial role beyond porosity alone.

Keywords: lattice-like scaffolds, bioengineering, mechanical properties, porosity

1. INTRODUCTION

Bone scaffolds are widely used to provide mechanical support and structural integrity in cases of bone defects or large tissue loss. These scaffolds serve two primary functions: to mimic the mechanical properties of the surrounding bone in order to maintain the physiological load-bearing balance and prevent complications such as stress shielding or implant failure, and to promote bone

regeneration by incorporating bioactive materials that stimulate new tissue growth. This study focuses exclusively on the mechanical behaviour of the scaffold.

Scaffold designs are typically categorized into two main groups [1]: porous scaffolds (Figure 1 - left), which emulate the morphology of cancellous bone, and lattice-like scaffolds (Figure 1 - right), which adopt more geometrically regular structures. In porous scaffolds, the design emphasis is placed on the

pore geometry—specifically the shape, size, and distribution of the voids. The connecting elements serve primarily to define and support these voids and are often formed as complex shell-like structures. In contrast, lattice-like scaffolds shift the design focus from the pores to the structural elements themselvescommonly referred to as struts. While latticelike scaffolds also occupy a largely void-filled volume, their open and interconnected nature may in some cases allow for even greater permeability and airiness than porous scaffolds. However, due to the reduced surface area of the structural elements, the contact interface with the surrounding tissue may be significantly smaller compared to that of porous scaffolds.





Figure 1. Porous (left) and lattice-like (right) bone scaffold structures

While porous scaffold designs dominate the lattice-based concepts literature, comparatively underexplored, primarily due to their more complex and time-consuming design procedures. Various computer-aided design (CAD) strategies have been employed in scaffold modelling. One common approach involves the use of unit cells micro-architectural elements that are replicated and assembled into a complete macrostructure [2, 3]. Alternatively, monolithic macro-scale designs can be created directly as a unified scaffold structure, [4, 5]. Both approaches can utilize different modelling techniques. For instance, scaffold geometry can be generated through Boolean operations, by subtracting predefined shapes from a base volume [2, 6], or by applying wireframe-based design principles, where struts define the structure's topology, [2, 4]. Furthermore, topology optimization techniques have been used to adapt scaffold geometry to

specific loading and boundary conditions, enhancing structural performance.

Across multiple studies [4, 6, 7, 8], several recurring design parameters have been identified, regardless of the specific modelling approach. These include:

- Pore size or strut diameter,
- Pore density or number of struts,
- Strut orientation or angle, and
- Overall scaffold dimensions (e.g., height, width, diameter).

Although the choice of design methodology (whether the scaffolds are based on unit cells, macro-scale volumes, or patient-specific customization) introduces variability in scaffold geometry, these global design parameters consistently influence the scaffold's mechanical and biological performance.

To ensure clinical applicability, scaffolds must meet specific mechanical performance requirements. Numerous experimental studies have assessed the mechanical behaviour of porous scaffolds through uniaxial compression testing [7, 9] while others have employed computational structural analysis methods to simulate scaffold behaviour under loading conditions [2, 9, 10]. These investigations have revealed key trends regarding the influence of both geometrical parameters [6, 9] and manufacturing conditions [8, 10] on overall mechanical response.

As highlighted in the literature review, further investigation of lattice-like scaffolds is needed, and particularly of those featuring free-form and custom-made geometries. These complex designs, although promising, remain insufficiently explored in terms of their mechanical behaviour and practical application. One such scaffold design, developed and presented by the authors in a previous study [11], was specifically designed to address the challenges of large segmental defects in long bones (Figure 2). This structure features a tailored lattice configuration optimized for both anatomical compatibility and load-bearing capacity.



Figure 2. Custom lattice like scaffold

The present study builds upon earlier work of the authors as part of an ongoing research efforts focused on evaluating and optimizing the aforementioned scaffold design. The objective of this paper is to investigate the relationship between scaffold porosity and its mechanical performance, with the aim of establishing general design principles that can guide the development of structurally efficient and clinically viable lattice-like bone scaffolds.

2. METHODOLOGY

The custom lattice-like scaffold models described in the previous section were subjected to uniaxial compression testing to evaluate their mechanical performance. A total of 12 scaffold samples were fabricated, each featuring a distinct porosity level. The underlying CAD model was fully parametrized, enabling systematic variation of key geometrical features. By adjusting the following parameters:

- outer strut diameter,
- inner strut diameter,
- outer strut angle,
- inner strut angle, and
- number of outer struts,

twelve unique scaffold configurations were generated, each with a different porosity percentage. These configurations served as the basis for analysing the influence of scaffold porosity on its mechanical behaviour. An overview of the tested designs and their respective porosity values is provided in Table 1 and presented in Figure 3.

Table 1. Scaffold samples and their respective porosity values

#	Porosity	#	Porosity
1	76.01	7	74.18
2	82.68	8	79.78
3	78.47	9	83.83
4	80.32	10	77.41
5	86.33	11	83.28
6	79.68	12	76.85



Figure 3. Custom lattice like scaffold used for the experiments

Machine used for fabrication of the above-mentioned scaffolds was EOS Formiga P100 (Figure 4). It has the build volume of 200 x 250 x 330 mm and layer resolution from 100 micron to 60 micron. As scaffold material, PA2200 – polyamide 12 was used (PA12) (Table 2 provides some information about this material).



Figure 4. EOS Formiga P100 SLS 3D printer

Table 2. Material properties of PA12

Property	Value		
Material type	Polyamide 12 (PA12)		
Manufacturing process	Selective Laser		
	Sintering (SLS)		
Color	White		
Tensile strength	~48 MPa		
Elongation at break	~20%		
Young's modulus	~1650 MPa		
Density	~930 kg/m³ (solid)		
Heat deflection	~95 °C (at 1.8 MPa)		
temperature			

Quasi-static uniaxial compression tests were carried out on Shimadzu Table-top AGS-X universal testing machine with a 10 kN load cell (the load cell accuracy is within ±0.5% of the indicated test force, for forces between 20 N and 10 kN). During the tests, a crosshead speed of 1 mm/min was used (with a speed accuracy of 0.1%). The force-stroke points were collected with the Shimadzu TrapeziumX software with a 100 Hz frequency. The illustration of the machine and testing setup is presented in Figure 5. To ensure accurate and reliable measurements, custom-made compression plates were fabricated specifically for this study. The plates were manufactured from high-strength steel, significantly stronger than the PA12 material used for the scaffolds, in order to eliminate any deformation of the fixtures during testing and to preserve the integrity of the experimental data.



Figure 5. Shimadzu Table-top AGS-X 10 kN universal testing machine (left), experiment setup (right)

The experimental output obtained from the compression tests consisted of force—displacement

curves. For each scaffold configuration, three independent tests were performed to ensure the reliability and repeatability of the results.

3. RESULTS AND DISCUSION

Figure 6 presents the force—displacement curves obtained during the second set of experimental trials for all tested specimens. The corresponding numerical results are summarized in Table 3, which lists the maximum force values recorded during testing for all twelve scaffold configurations, across all three repeated trials. Additionally, the table presents the average maximum force calculated from the three measurements for each individual scaffold design.

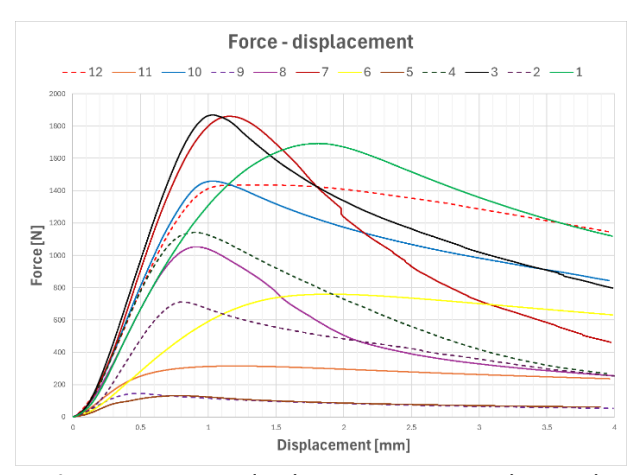


Figure 6. Force - displacement curves obtained during the second set of experimental trials

The curves (Figure 5) show noticeable differences in both maximum force and postpeak behaviour, which directly correlate with scaffold geometry and porosity. Scaffolds with lower porosity (e.g., samples 3 and 7) exhibit steeper initial slopes, indicating stiffness, and reach significantly higher peak forces before failure. In contrast, high-porosity scaffolds (e.g., samples 2, 5 and 11) display a more gradual force increase, lower peak forces, and an earlier onset of deformation, reflecting reduced load-bearing capacity. The shape of the curves after peak force also varies considerably. Some configurations samples 12 and 6) maintain relatively high residual load capacity after peak force, suggesting a more gradual failure mode. Others

(e.g., samples 4 and 3) experience an abrupt load drop. These differences can be attributed not only to porosity but also to strut orientation, connection density, and load path continuity within the lattice structure.

Table 3. Maximum force values recorded during testing for all twelve scaffold configurations, across all three repeated trials

#	Porosity (%)	Fmax1 (N)	Fmax2 (N)	Fmax3 (N)	Average F (N)
1	76.01	1620.002	1691.573	1784.6	1698.725
2	82.68	539.1614	711.5094	743.38	664.6836
3	78.47	1879.869	1868.281	1563.94	1770.697
4	80.32	1335.344	1141.326	1653.7	1376.79
5	86.33	317.9026	131.6341	259.107	236.2146
6	79.68	968.0668	759.2185	859.218	862.1678
7	74.18	2813.004	1859.703	2590.22	2420.976
8	79.78	876.6985	1052.397	1433.87	1120.989
9	83.83	299.2614	145.9026	239.433	228.199
10	77.41	1674.898	1459.061	1468.97	1534.31
11	83.28	220.3528	315.0161	226.563	253.9773
12	76.85	975.0255	1434.867	1388.65	1266.181

The maximum force values obtained for all twelve scaffold configurations are summarized in Table 3. The results reveal a clear negative correlation between porosity and maximum compressive force (which can also be seen in Figure 7), where scaffolds with lower porosity generally exhibit higher load-bearing capacity. For example, the specimen with 74.18% achieved the highest porosity average maximum force (2420.976 N), while the most configuration (86.33% porosity) demonstrated the lowest mechanical strength (236.2146 N on average). However, the data also indicate that porosity alone does not fully determine mechanical performance. Certain scaffolds with very similar porosity values exhibited large differences in their maximum load capacity. For instance, the two samples with porosity levels of 76.01% and 76.85% showed average maximum forces of 1698.725 N and 1266.181 N, respectively, a difference of over 400 N. This suggests that other geometrical factors, such as strut arrangement, diameter, and orientation, play a significant role

in defining the overall mechanical response. It is also notable that some mid-range porosity designs (e.g., 78.47%) outperformed certain lower-porosity scaffolds (e.g., 77.41% and 76.85%), again highlighting that structural topology and load distribution within the lattice network can offset the expected loss of strength due to increased void fraction.

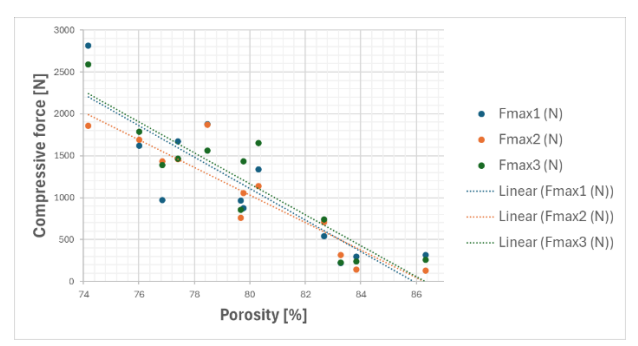


Figure 7. Correlation between porosity and maximum compressive force

4. CONCLUSION

This study investigated the relationship between porosity and mechanical performance of custom-designed lattice-like bone scaffolds, specifically tailored for large segmental defects in long bones. Twelve scaffold configurations with varying porosity levels were fabricated using SLS additive manufacturing and tested under uniaxial compression.

results confirmed theoretical expectations of a general decrease in strength with increasing porosity. However, the findings demonstrated that geometrical optimization at the strut and cell level can produce scaffolds with a large mechanical strength even at relatively high porosity levels. Furthermore, analysis of the force–deformation curves revealed that certain lattice designs are capable of retaining a portion of their loadbearing capacity even after the onset of structural failure. This characteristic may be advantageous in biomedical applications, where controlled failure and gradual load transfer to the surrounding bone tissue can facilitate the healing process and reduce the risk of catastrophic implant failure. However, there is a possibility that following unloading and subsequent reloading, these scaffolds may also experience immediate failure. This aspect warrants further investigation and will be the subject of future research.

Future work will focus on more detailed stress—strain characterization, accounting for complex and variable cross-sections, and on exploring topological optimization methods to further refine scaffold performance for specific clinical requirements. Additionally, given the complexity of the stress distribution within lattice-like scaffolds, incorporating finite element analysis (FEA) will be essential for accurately assessing the internal stress state and identifying potential failure zones.

ACKNOWLEDGEMENT

The research activities are financed by the Ministry of Science, Technological Development and Innovation of the Republic of Serbia (Contract No. 451-03-47/2023-01/200109).

REFERENCES

- [1] J. Milovanović, M. Stojković, M. Trifunović, and N. Vitković, "Review of Bone Scaffold Design Concepts and Design Methods," Facta Univ. Ser. Mech. Eng., 2020.
- [2] M. A. Wettergreen, B. S. Bucklen, B. Starly, E. Yuksel, W. Sun, and M. A. K. Liebschner, "Creation of a unit block library of architectures for use in assembled scaffold engineering," Comput. Des., vol. 37, no. 11, pp. 1141–1149, Sep. 2005.
- [3] R. M. Gorguluarslan, S. K. Choi, and C. J. Saldana, "Uncertainty quantification and validation of 3D lattice scaffolds for computer-aided biomedical applications," J. Mech. Behav. Biomed. Mater., vol. 71, pp. 428–440, Jul. 2017.
- [4] M. S. Stojkovic, N. D. Korunovic, M. D. Trajanovic, J. R. Milovanovic, M. B. Trifunovic, and N. M. Vitkovic, "Design study of anatomically shaped lattice scaffolds for the bone tissue recovery," ECCOMAS Spec. Interes. Conf. SEECCM 2013 3rd South-East Eur. Conf.

- Comput. Mech. Proc. An IACM Spec. Interes. Conf., pp. 381–393, 2013.
- [5] S. Eshraghi and S. Das, "Micromechanical finite-element modeling and experimental characterization of the compressive mechanical properties of polycaprolactone—hydroxyapatite composite scaffolds prepared by selective laser sintering for bone tissue engineering," Acta Biomater., vol. 8, no. 8, pp. 3138–3143, Aug. 2012
- [6] C. Shi, N. Lu, Y. Qin, M. Liu, H. Li, and H. Li, "Study on mechanical properties and permeability of elliptical porous scaffold based on the SLM manufactured medical Ti6Al4V," PLoS One, vol. 16, no. 3, p. e0247764, Mar. 2021.
- [7] G. E. Ryan, A. S. Pandit, and D. P. Apatsidis, "Porous titanium scaffolds fabricated using a rapid prototyping and powder metallurgy technique," Biomaterials, vol. 29, no. 27, pp. 3625–3635, Sep. 2008.
- [8] S. Cahill, S. Lohfeld, and P. E. McHugh, "Finite element predictions compared to experimental results for the effective modulus of bone tissue engineering scaffolds fabricated by selective laser sintering," J. Mater. Sci. Mater. Med. 2009 206, vol. 20, no. 6, pp. 1255– 1262, Feb. 2009.
- [9] M. Ramu, M. Ananthasubramanian, T. Kumaresan, R. Gandhinathan, and S. Jothi, "Optimization of the configuration of porous bone scaffolds made of Polyamide/Hydroxyapatite composites using Selective Laser Sintering for tissue engineering applications," Biomed. Mater. Eng., vol. 29, no. 6, pp. 739–755, Jan. 2018.
- [10] G. Ryan, P. McGarry, A. Pandit, and D. Apatsidis, "Analysis of the mechanical behavior of a titanium scaffold with a repeating unit-cell substructure," J. Biomed. Mater. Res. Part B Appl. Biomater., vol. 90B, no. 2, pp. 894–906, Aug. 2009.
- [11] R. Turudija, J. Arandjelovic, M. Stojkovic, N. Korunovic, J. Milovanovic, "Novel approach to generic parametrized lattice scaffold model design", Conference ICIST 2022, Kopaonik, Serbia.